

COMPARISON OF NUMERICAL METHODS IN THE CONTRAST IMAGING PROBLEM IN NMR

Bernard Bonnard, Mathieu Claeys, Olivier Cots and Pierre Martinon

Abstract—In this article, the contrast imaging problem in nuclear magnetic resonance is modeled as a Mayer problem in optimal control. A first synthesis of locally optimal solutions is given in the single-input case using geometric methods and the HamPath software, both based on Pontryagin’s maximum principle. We then compare these results using direct methods implemented with the Bocop toolbox and a moment-based approach, making a first step towards global optimality.

INTRODUCTION

A classical problem in Nuclear Magnetic Resonance (NMR) spectroscopy is to control, using a magnetic field, a spin-1/2 particle in a dissipative environment whose dynamics is governed by the *Bloch equation* [12]

$$\begin{aligned}\frac{dM_x}{d\tau} &= -M_x/T_2 + \omega_y M_z - \Delta\omega M_y \\ \frac{dM_y}{d\tau} &= -M_y/T_2 - \omega_x M_z + \Delta\omega M_x \\ \frac{dM_z}{d\tau} &= (M_0 - M_z)/T_1 + \omega_x M_y - \omega_y M_x\end{aligned}\quad (1)$$

where the state variables correspond to the magnetization vector $M = (M_x, M_y, M_z)$, T_1 and T_2 are the relaxation rates, $\Delta\omega$ is the resonance offset and τ is the time. In this model the control is the magnetic field $\omega = (\omega_x, \omega_y, 0)$ which is bounded here by $|\omega| \leq \omega_{\max} = 32.3\text{Hz}$. In order to set the equilibrium of the free motion to $(0, 0, 1)$, we normalize the coordinates to $q = (x, y, z) = (M_x, M_y, M_z)/M_0$, such that q belongs to the Bloch ball $|q| \leq 1$. We then normalize the control by $u = \omega/\omega_{\max}$ and the normalized time is $t = \tau \omega_{\max}$. In this paper, we analyze the simplified model $\Delta\omega = 0$, where homogeneity of the magnetic fields is assumed, yielding the following normalized system

$$\begin{aligned}\frac{dx}{dt} &= -\Gamma x && + u_2 z \\ \frac{dy}{dt} &= -\Gamma y && - u_1 z \\ \frac{dz}{dt} &= \gamma(1 - z) && + u_1 y - u_2 x,\end{aligned}\quad (2)$$

B. Bonnard is with Institut de Mathématiques de Bourgogne, Université de Bourgogne, 9 avenue Alain Savary, 21078 Dijon, France, bernard.bonnard@u-bourgogne.fr

M. Claeys is with CNRS; LAAS; 7 avenue du colonel Roche, F-31077 Toulouse; France and with Université de Toulouse; UPS, INSA, INP, ISAE; UT1, UTM, LAAS; F-31077 Toulouse; France, mclaeys@laas.fr.

O. Cots is with INRIA Sophia Antipolis Méditerranée, 06902 Sophia Antipolis, France, olivier.cots@inria.fr.

P. Martinon is with Inria and Ecole Polytechnique, 91128 Palaiseau France, pierre.martinon@inria.fr.

where $\Gamma = 1/(\omega_{\max} T_2)$ and $\gamma = 1/(\omega_{\max} T_1)$. In the contrast problem, we consider two uncoupled spin-1/2 systems corresponding to different particles, each of them solutions of the Bloch equation (2) with respective damping coefficients, (γ_1, Γ_1) and (γ_2, Γ_2) and controlled by the same magnetic field. By denoting each system by $\frac{dq_i}{dt} = F_{\Lambda_i}(q_i, u)$, $\Lambda_i = (\gamma_i, \Gamma_i)$ and $q_i = (x_i, y_i, z_i)$ the magnetization vector for each spin particle, this leads to consider the system

$$\frac{dq_1}{dt} = F_{\Lambda_1}(q_1, u), \quad \frac{dq_2}{dt} = F_{\Lambda_2}(q_2, u)$$

which is written shortly as $\frac{dx}{dt} = F(x, u)$, where $x = (q_1, q_2)$ is the state variable.

The contrast problem by **saturation** is the following *optimal control problem (OCP)*: starting from the equilibrium point $x_0 = ((0, 0, 1), (0, 0, 1))$, reach in a given transfer time t_f the final state $q_1(t_f) = 0$ (corresponding to zero magnetization of the first spin, called saturation) while maximizing $|q_2(t_f)|^2$, the **contrast** being $|q_2(t_f)|$. The contrast problem can be stated as a *Mayer problem* given by the following smooth conditions:

- 1) A system $\frac{dx}{dt} = F(x, u)$, $x \in \mathbf{X} \subseteq \mathbb{R}^n$, with fixed initial state $x(0) = x_0$ and where the control belongs to the control domain \mathbf{U} . For the contrast problem

$$\mathbf{X} = \{x = (q_1, q_2) \in \mathbb{R}^n : |q_1| \leq 1, |q_2| \leq 1\},$$

$\mathbf{U} = \{u \in \mathbb{R} : |u| \leq 1\}$ and F is given by (2).

- 2) A terminal manifold to reach, defined by $f(x) = 0$, where $f : \mathbb{R}^n \rightarrow \mathbb{R}^k$. Here we have

$$\mathbf{X}_f = \{x = (q_1, q_2) \in \mathbb{R}^n : q_1 = 0, |q_2| \leq 1\} \subset \mathbf{X},$$

- 3) A cost to be minimized $\min_{u(\cdot)} c(x(t_f))$ where $c : \mathbb{R}^n \rightarrow \mathbb{R}$ is a regular mapping. Here c is the contrast.

In practical experiments, we consider two cases:

- a) The **bi-input case** where $x = (q_1, q_2) \in \mathbb{R}^6 \cap \mathbf{X}$ and $|u| = (u_1^2 + u_2^2)^{1/2} \leq 1$.
- b) The **single-input case** where the system is restricted to $x_1 = x_2 = 0$, the control field is restricted to the real field, i.e., $u_2 = 0$, and each spin is restricted to the plane $q_i = (y_i, z_i)$.

The use of particular pulse sequences (*i.e.* control law $u(\cdot)$) in the contrast problem is not new since this question was raised at the beginning of the development of Magnetic Resonance Imaging (MRI) in the seventies. Different strategies based on intuitive reasoning have been proposed such as the Inversion Recovery Sequence. Recently, S. J. Glaser

introduced the optimal control point of view [9] and analysed the problem in his group using an adapted numerical scheme (the GRAPE algorithm [8]). A different approach based on Pontryagin's Maximum Principle was recently used to select minimizers in the single input case [5]. This leads to a numerical investigation described in [6] using the `HamPath`¹ software, based on indirect methods: shooting and differential continuation.

One objective of this article is to compare these results with a direct method implemented with the `Bocop`² toolbox [2]. This approach relies on a time discretization of the state and control variables, with the resulting nonlinear programming problem solved by interior point techniques. Direct methods are typically easier to initialize than indirect methods, however their solutions tend to be coarser. Direct methods fall in the classe of local optimization, like indirect approaches.

A distinguishing feature of the contrast problem are its many locally optimal solutions, which can be computed by the previously described direct and indirect methods. An important question is then to assert their **global optimality**. The second objective of this paper is to use a moment/Linear Matrix Inequality (`lmi`) technique [7], [11] to compute such an estimate. In fact, the method allows to build a hierarchy of relaxations of the original problem, each in the form of a convex `lmi` problem. Because of this convexity, the relaxations can be solved readily without requiring an initial guess (we used `SeDuMi` [13]) and provide lower bounds on the true cost.

The paper is organized in three sections. The first one settles the necessary conditions for the contrast problem. The second details the three numerical methods used in the third section, which presents the results in the single-input case.

I. NECESSARY OPTIMALITY CONDITIONS

See [5] for the detailed theoretical framework.

A. Maximum principle

Proposition 1. *If u^* with corresponding trajectory x^* is optimal then the following necessary optimality conditions are satisfied. Denoting $H(x, p, u) = \langle p, F(x, u) \rangle$ as the pseudo-Hamiltonian, there exists $p^*(\cdot)$ such that for almost every $t \in [0, t_f]$,*

- (i) $\frac{dx^*}{dt} = \frac{\partial H}{\partial p}(x^*, p^*, u^*), \quad \frac{dp^*}{dt} = -\frac{\partial H}{\partial x}(x^*, p^*, u^*)$
- (ii) $H(x^*, p^*, u^*) = \max_{v \in U} H(x^*, p^*, v)$

and the following boundary conditions

- (iii) $f(x^*(t_f)) = 0$
- (iv) $p^*(t_f) = p^0 \frac{\partial c}{\partial x}(x^*(t_f)) + \sum_{i=1}^k \sigma_i \frac{\partial f_i}{\partial x}(x^*(t_f)), \quad \sigma = (\sigma_1, \dots, \sigma_k) \in \mathbb{R}^k, \quad p^0 \leq 0$ (transversality condition)

Definition 1. *The solutions of conditions (i) and (ii) of Prop. 1 are called extremals and BC-extremals if they satisfy the Boundary Conditions (iii) and (iv).*

¹<http://cots.perso.math.cnrs.fr/hampath>

²<http://bocop.org>

B. Application to the contrast problem

State space: The Bloch ball is invariant for the dynamics of each spin, thus the state constraints can be omitted for analysis, and the maximum principle can be applied.

Boundary conditions: In the contrast problem, $x = (q_1, q_2)$, $f = 0$ is the set $q_1 = 0$, and the cost to minimize is $c(x) = -|q_2|^2$. Hence, splitting the adjoint vector into $p = (p_1, p_2)$, we deduce from the transversality condition that $p_2(t_f) = -2p^0 q_2(t_f)$, $p^0 \leq 0$. If p^0 is nonzero, it can be normalized to $p^0 = -1/2$.

Extremal curves in the Bi-input case: The system is written as $\frac{dx}{dt} = F_0(x) + u_1 F_1(x) + u_2 F_2(x)$, $|u| \leq 1$ and the maximization condition in Prop. 1 leads to the following parameterization of the extremal controls:

$$u_1 = \frac{H_1}{\sqrt{H_1^2 + H_2^2}}, \quad u_2 = \frac{H_2}{\sqrt{H_1^2 + H_2^2}},$$

where $H_i = \langle p, F_i(x) \rangle$ are Hamiltonian lifts outside the switching surface $\Sigma : H_1 = H_2 = 0$. Plugging such a u into the pseudo-Hamiltonian gives the *true Hamiltonian* $H_n = H_0 + (H_1^2 + H_2^2)^{1/2}$. The smooth solutions of the corresponding vector field are called *extremals of order zero*.

Extremal curves in the the single-input case: Consider the case where the control is restricted to a single input and the system is written $\frac{dx}{dt} = F(x) + uG(x)$, where x belongs to a 4-dimensional space \mathbf{X} and $|u| \leq 1$. We denote H_F and H_G to be the respective Hamiltonian lifts.

Applying the maximization condition, there are two types of extremals.

- Regular extremals: The control is given by $u(t) = \text{sgn}H_G(z(t))$, $z = (x, p)$. If the number of switchings is finite, it is called bang-bang.
- Singular extremals: Since the system is linear in u , the maximization condition leads, in the singular case, to the condition $H_G(z(t)) = 0$, with the control

$$u_s = -\frac{\{\{H_G, H_F\}, H_F\}}{\{\{H_G, H_F\}, H_G\}}, \quad (3)$$

where $\{\cdot, \cdot\}$ is the standard Poisson bracket.

According to the maximum principle, an optimal solution is the concatenation of bang and singular arcs and the complexity of this sequence is measured by the number of concatenated arcs. This leads to the following lemma:

Lemma 1. *In the contrast problem, the simplest BC-extremal is of the form BS, i.e a Bang arc followed by a Singular arc.*

A straightforward computation gives the following result.

Proposition 2. *The extremals of the single-input case are extremals of the bi-input case.*

A limit case in the contrast problem is the case where the transfer time t_f is exactly the time T_{\min} to transfer the first spin to zero, the optimal control producing a final contrast $|q_2(T_{\min})|$. We have the following proposition

Proposition 3. *The time-minimal solution of the first spin system can be embedded as an extremal solution of the contrast problem with $p^0 = 0$ in the transversality condition of Prop. 1.*

Optimal solution structure. In the single-input case, the geometrical study of the contrast problem ensures that the optimal solution is a concatenation of bang and singular arcs ([6], [4]). We note nBS a structure composed by n Bang-Singular sequences. The optimal sequence is not known and must be identified.

II. NUMERICAL METHODS

In this section we present the three numerical methods used for the resolution of the contrast problem.

A. HamPath

The HamPath ([6]) software implements an indirect method based on shooting, differential continuation, and variational equations. We give in this section a summary of the principles used to solve the contrast problem in the single-input case, excerpted from [4], [6]. First we use the following regularization to detect the BS-sequences and find a good approximation of the solution:

$$c(x(t_f)) + (1 - \lambda) \int_0^{t_f} |u|^{2-\lambda} dt, \quad \lambda \in [0, 1],$$

with fixed final time t_f . The regularized Hamiltonian is

$$H(x, p, \lambda) = p^0(1 - \lambda)|u(\cdot)|^{2-\lambda} + H_F(x, p) + u(\cdot) H_G(x, p),$$

where $u(\cdot)$ stands for $u(x, p, \lambda)$ and

$$u(x, p, \lambda) = \text{sgn}(H_G(x, p)) \left(\frac{2|H_G(x, p)|}{(2 - \lambda)(1 - \lambda)} \right)^{\frac{1}{1-\lambda}}.$$

The homotopic function $h : \Omega \subset \mathbb{R}^n \times [0, 1] \rightarrow \mathbb{R}^n$ given by the transversality conditions is

$$h(p_0, \lambda) = \begin{pmatrix} q_1(t_f, x_0, p_0, \lambda) \\ q_2(t_f, x_0, p_0, \lambda) - p_2(t_f, x_0, p_0, \lambda) \end{pmatrix},$$

where $x_0 = ((0, 1), (0, 1))$ is the initial state and p_0 is the initial adjoint vector. We first solve $h(p_0, \lambda)|_{\lambda=0} = 0$ and then use differential continuation to get the initial adjoint vector for $\lambda_f = 1 - \varepsilon$. We use the solution at λ_f to solve the contrast problem ($\lambda = 1$) by multiple shooting. Finally, we use the homotopy method again to study the behavior of the solutions regarding to the parameter t_f .

An important issue in the contrast problem is to deal with the many local solutions, such that, for a given value \bar{t}_f of the parameter, we must compare the cost associated to each component of $\{h = 0\} \cap \{t_f = \bar{t}_f\}$, where each branch of $\{h = 0\}$ is called a path of zeros. This global aspect is responsible for a possible loss of regularity on the value function $t_f \mapsto c(x(t_f))$ and on the globally optimal path of zeros.

B. Bocop

The so-called direct approach transforms the infinite dimensional optimal control problem (OCP) into a finite dimensional optimization problem (NLP). This is done by a discretization in time applied to the state and control variables, as well as the dynamics equation. These methods are usually less precise than indirect methods based on Pontryagin's Maximum Principle, but more robust with respect to the initialization. Also, they are more straightforward to apply, hence their wide use in industrial applications.

Summary of the time discretization:

$$\begin{array}{ll} t \in [0, t_f] & \rightarrow \{t_0 = 0, \dots, t_N = t_f\} \\ z(\cdot), u(\cdot) & \rightarrow X = \{z_0, \dots, z_N, u_0, \dots, u_{N-1}, t_f\} \\ \text{Criterion} & \rightarrow \min c(z_N) \\ \text{Dynamics} & \rightarrow (\text{ex : Euler}) z_{i+1} = z_i + hf(z_i, u_i) \\ \text{Adm. Cont.} & \rightarrow -1 \leq u_i \leq 1 \\ \text{Bnd. Cond.} & \rightarrow \Phi(z_0, z_N) = 0 \end{array}$$

We therefore obtain a nonlinear programming problem on the discretized state and control variables

$$(NLP) \begin{cases} \min F(z) = c(z_N) \\ LB \leq C(z) \leq UB \end{cases}$$

All tests were run using the Bocop software [2]. The discretized nonlinear optimization problem is solved by the well-known IPOPT solver [14] with MUMPS [1], while the derivatives are computed by sparse automatic differentiation.

C. lmi

The moment approach is a global optimization technique that transforms a non-linear, possibly infinite-dimensional optimization problem into convex, finite-dimensional relaxations in the form of Linear Matrix Inequalities (LMI). We follow [11] for the specific case of optimal control with bounded controls and [10] for the main steps of the method.

The first step is to embed problem (OCP) into a Linear Program (LP) on measures, by the use of so called occupation measures encoding admissible trajectories. For each admissible control $u(t)$, define its corresponding *time occupation measure* $\mu[u(t)] \in \mathcal{M}^+(\mathbf{K} := [0, t_f] \times \mathbf{U} \times \mathbf{X})$, a positive Radon measure, as:

$$\mu[u(t)](\mathbf{A}, \mathbf{B}, \mathbf{C}) := \int_{[0, t_f] \cap \mathbf{A}} \delta_{u(t)}(\mathbf{B}) \delta_{x[u(t)](t)}(\mathbf{C}) dt.$$

Here, δ_{x^*} is the Dirac measure located at x^* , and \mathbf{A} , \mathbf{B} and \mathbf{C} are Borel subsets of resp. $[0, t_f]$, \mathbf{U} and \mathbf{X} . That is, $\mu[u(t)]$ measures the time "spent" by the admissible triplet $(t, u(t), x[u(t)](t))$ on Borel subsets of \mathbf{K} . Similarly, we define the final state occupation measure $\mu_f[u(t)] \in \mathcal{M}^+(\mathbf{X}_f)$ for the same admissible control as:

$$\mu_f[u(t)](\mathbf{C}) := \delta_{x[u(t)](t_f)}(\mathbf{C}).$$

Proposition 4 (Measure embedding). *Control problem (OCP) can be reformulated equivalently in terms of occupation measures:*

$$J_\mu = \inf_{\mu[u(t)], \mu_f[u(t)]} \langle c(\cdot), \mu_f[u(t)] \rangle \quad (4)$$

such that, $\forall v(t, x) \in \mathcal{C}^1([0, t_f] \times \mathbf{X})$,

$$\langle v(t_f, \cdot), \mu_f[u(t)] \rangle - v(0, x_0) = \left\langle \frac{\partial v}{\partial t} + \frac{\partial v}{\partial x} \cdot F, \mu[u(t)] \right\rangle. \quad (5)$$

That is, $J_\mu = J_{\text{OCP}}$ the original criterion of (OCP).

Consider the following relaxation of problem (4)-(5), where the decision variables are now any measure $\mu \in \mathcal{M}^+(\mathbf{K})$ and $\mu_f \in \mathcal{M}^+(\mathbf{X}_f)$, instead of occupation measures generated by admissible controls:

$$J_{\text{LP}} = \inf_{\mu, \mu_f} \langle c(\cdot), \mu_T \rangle \quad (6)$$

such that, $\forall v(t, x) \in \mathcal{C}^1([0, t_f] \times \mathbf{X})$,

$$\langle v(t_f, \cdot), \mu_f \rangle - v(0, x_0) = \left\langle \frac{\partial v}{\partial t} + \frac{\partial v}{\partial x} \cdot F, \mu \right\rangle. \quad (7)$$

In ill-posed problems, there could be a strict gap induced by the relaxation, i.e. $J_{\text{LP}} < J_\mu$, but for the problem at hand, we have the following result:

Proposition 5 (No relaxation gap).

$$J_{\text{LP}} = J_\mu$$

Proof. The set of admissible vector fields for dynamics F is convex for any $x \in \mathbf{X}$, such that theorem 3.6 (ii) of [11] holds. \square

Unfortunately, there is no generic tractable method to solve LP problem (6)-(7), and additional structure on problem data is required. For optimal control problem (OCP), this structure is provided by the polynomial cost and dynamics, as well as the basic semi-algebraic characterization of the compact sets \mathbf{X} and \mathbf{X}_f . It is then possible to manipulate measures by their moments in a given polynomial basis, which yields a Semi-Definite Program (SDP) on countably many moments, with cost $J_{\text{SDP}} = J_{\text{LP}}$. Truncation of those moment sequences up to degree $2d$ yields the order d relaxation in the form of a tractable LMI problem, with cost J_{LMI}^d . These LMI relaxations yield tighter lower bounds on the true cost as relaxation order is increased, converging monotonically to the solution of (OCP), i.e.

Proposition 6 (Monotone convergence).

$$\lim_{n \rightarrow \infty} J_{\text{LMI}}^n \uparrow J_{\text{SDP}} = J_{\text{LP}} = J_\mu = J_{\text{OCP}}$$

The passage from (6)-(7) to a given LMI relaxation can be fully automated using the GLOPTIPOLY toolbox [7]. The strong feature of the method is that those LMIs generate lower bounds on the true cost, and can therefore be used as certificates of global optimality. The weak points of the method are its poor algorithmic complexity for unstructured problem, and in the case of optimal control, the unavailability of a generic method to recover controls.

III. NUMERICAL SIMULATIONS, SINGLE-INPUT CASE

We present here the results about the single-input case. From the experimental point of view we are interested in the following cases, the parameters being the relaxation times given in seconds.

a) **Fluid case.**

Spin 1: Cerebrospinal fluid: $T_1 = 2, T_2 = 0.2$;

Spin 2: Water: $T_1 = 2.5 = T_2$.

b) **Blood case.**

Spin 1: Deoxygenated blood: $T_1 = 1.35, T_2 = 0.05$;

Spin 2: Oxygenated blood: $T_1 = 1.35, T_2 = 0.2$.

In both cases the contrast problem has many local solutions, sometimes with different control structures (meaning the number of Bang-Singular sequences). The structure of the best policy can change depending on the final time, as detailed below in III-A and Fig. 1, see [6] for full details.

A. HamPath

The results presented in the following part are excerpted from [6]. We give the synthesis of locally optimal solutions obtained in the blood and fluid cases. For the blood, we show on Fig. 1 (left) the contrast for five different components of $\{h = 0\}$, for final times $t_f \in [1, 2]T_{\text{min}}$. The three black branches are made only of BS solutions while the two others are made of 2BS and 3BS solutions. For maximizing the contrast, the best policy, drawn as solid lines, is: BS for $t_f \in (1, 1.294)T_{\text{min}}$ and 3BS for $t_f \in (1.294, 2]T_{\text{min}}$. In the special case $t_f = T_{\text{min}}$, the solution is 2BS. For the fluid, on Fig. 1 (right), we represent four different branches with 2BS and 3BS solutions. The greatest two value functions intersect around $t_f = 1.035T_{\text{min}}$ and the best policy (solid lines) switches between 2BS and 3BS strategies.

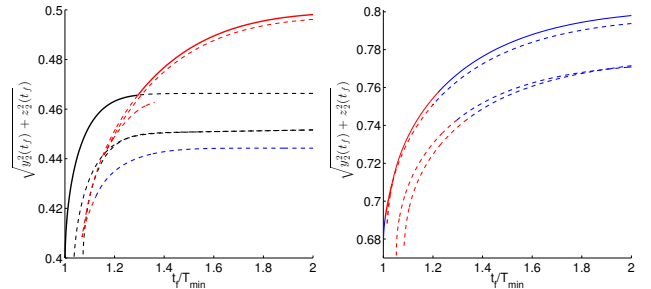


Fig. 1: **HamPath.** Illustration of local solutions (each branch corresponds to a control structure). Best policy as solid lines, local solutions as dashed lines. Blood and Fluid cases.

We now compare these results with the direct and LMI methods, in order to assess the optimality of these two sub-optimal synthesis.

B. Bocop

We present here the results for the direct approach. The only a priori information is the value of the minimum time transfer from [6], used to set the final time in the $[T_{\text{min}}, 2T_{\text{min}}]$ range. The state and control variables are

initialized as constant functions, with the values $y_1(\cdot) = 0$, $z_1(\cdot) = 0.5$, $y_2(\cdot) = 0$, $z_2(\cdot) = 1$, and $u_x(\cdot) = 0.1$. Each optimization uses this same initial point, and there is no continuation applied here. The discretization methods used are 4th order Gauss or 6th order Lobatto, with 500 to 1000 time steps depending on the problem.

Overall comparison. We show on Fig. 2 the solutions found with `Bocop` plotted over the branches identified with `HamPath` in [6]. In most cases the direct solutions belong to one of the already found branches, although some additional branches seem to appear as well. This confirms the complex structure of the extremals for this problem, with several families of local solutions. However, no new solutions with a better contrast were found, which suggests the practical validity of the continuation strategy used with `HamPath`.

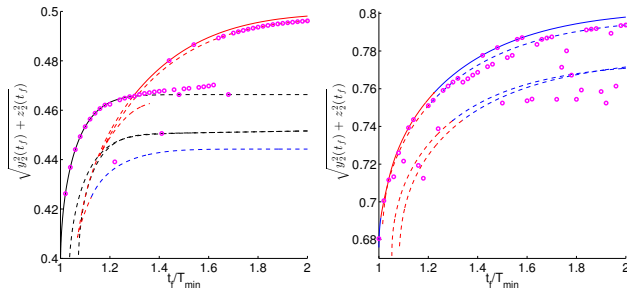


Fig. 2: `Bocop` and `HamPath`: Blood and Fluid cases.

Blood case. Depending on the final time, we find solutions with either structure BS or 3BS. For small values of t_f , `Bocop` converges to the optimal solution found by `HamPath`, but for larger t_f it tends to miss the branch of optimal solutions, see Fig. 2. On Fig. 3 we show the `Bocop` and `HamPath` solutions for $t_f = 1.1T_{\min}$. The trajectories for the two spins are identical, and the control is the same, with the exception of some oscillations at the end of the direct solution. These oscillations actually average the "correct" control (recall that the system is linear in the control).

Fluid case. The situation in the fluid case is a bit more complicated, and `Bocop` converges rather randomly to solutions on different branches, either BS or 3BS. We show on Fig. 4 the solutions for $t_f = 1.5T_{\min}$, where `Bocop` actually finds the best known structure. We observe that both solutions are extremely close, save for a few isolated spikes in the control at the switching times.

Initializing `HamPath` from `Bocop`. We pick now one case where `Bocop` converges to the best known solution, and try to use it to initialize `HamPath`. We recover the control structure, the switching times t_i , and the $x(t_i), p(t_i)$ (we recall that p corresponds to the multipliers for the discretized dynamics in (*NLP*)). This initialization permitted the convergence of the shooting method, without resorting to continuation techniques. Table I compares the two solutions

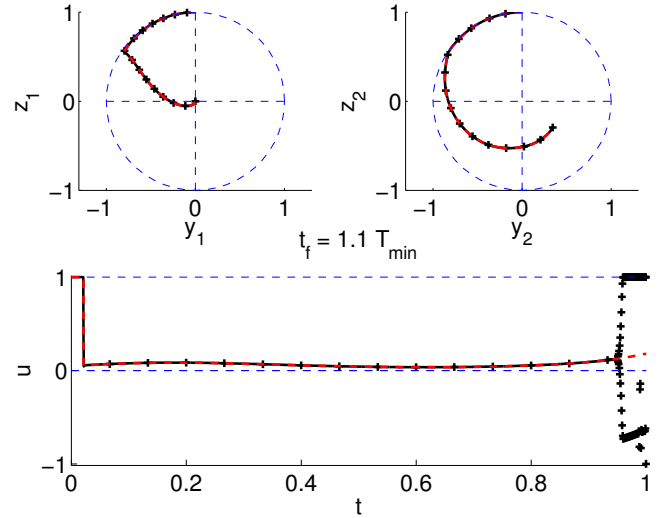


Fig. 3: `Bocop` and `HamPath`: Blood case, $t_f = 1.1T_{\min}$

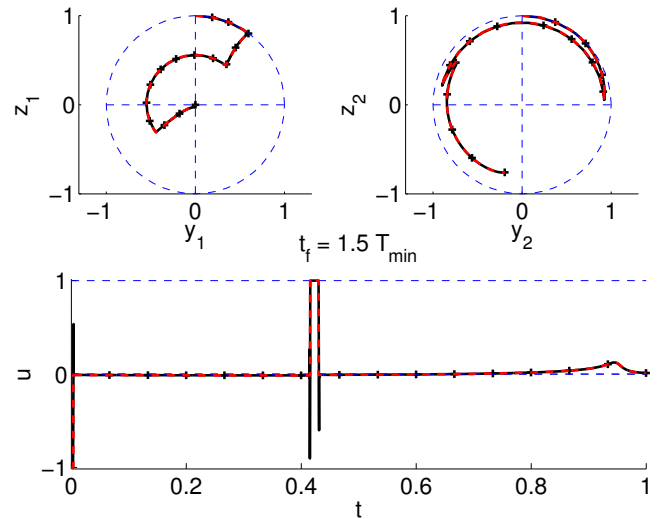


Fig. 4: `Bocop` and `HamPath`: Fluid case, $t_f = 1.5T_{\min}$

in the blood case, for $T_f = 1.1T_{\min}$ and $T_f = 1.54T_{\min}$. We see that the contrast and switching times are extremely close, and also check that the relative difference between the renormalized adjoint vector $p(0)$ and the corresponding multipliers is often small, and never exceeds 50%.

TABLE I: `Bocop` / `HamPath` comparison (Blood case).

t_f	Method	Contrast	Switching times t_i/t_f
$1.1T_{\min}$	<code>HamPath</code>	0.453	0.0211
	<code>Bocop</code>	0.453	0.02
$1.54T_{\min}$	<code>HamPath</code>	0.487	(0.005,0.348,0.395,0.814,0.855)
	<code>Bocop</code>	0.487	(0.004,0.349,0.394,0.815,0.853)

t_f	$\Delta p(0)$ between <code>Bocop</code> and <code>HamPath</code>
$1.1T_{\min}$	(9.81%, 3.45%, 33.75%, 0.61%)
$1.54T_{\min}$	(1.1%, 49.37%, 29.62%, 1.68%)

C. *lmi*

We apply now the *lmi* method to the contrast problem, in order to obtain upper bounds on the true contrast. Comparing these bounds to the contrast of our solutions then gives an insight about their global optimality.

Table II shows the evolution of the upper bound on the contrast in function of LMI relaxation order for the blood case with $t_f = T_{\min}$. The first relaxation gives the trivial upper bound, while higher orders yield a monotonically non-increasing sequence of sharper bounds, as expected. Relaxations of orders 5 and 6 yield very similar bounds, but this should not be interpreted as a termination criterion for the *lmi* method. Table II also shows the evolution of the number of decision variables involved in each LMI relaxation (before any eventual substitution) and the computational load. For all practical purposes, further results from the *lmi* method were limited to the fifth relaxation given the prohibitive computational load of the sixth one.

TABLE II: *lmi*: Upper bound on contrast (Blood case)

order	Upper bound	Nb. variables	CPU (s)
1	1.0000	49	1
2	0.6092	336	2
3	0.5877	1386	9
4	0.5400	4290	265
5	0.4577	11011	5147
6	0.4442	24752	63613

Fig. 5 compares the evolution of the upper bounds for different values of $t_f \in [T_{\min}, 2T_{\min}]$ with the best solutions found by *HamPath*. Also represented is the relative gap between the methods defined as $(C_{LMI} - C_H)/C_H$, where C_{LMI} is the *lmi* upper bound and C_H is the contrast found with *HamPath*. At the fifth relaxation, the average gap is 11%, which given the application is satisfactory on the experimental level. Fig. 6 shows the same results for the fluid case. Here, the relative gap on the contrast is about 1% at the fifth relaxation, which strongly suggest that the solution is actually a global optimum.

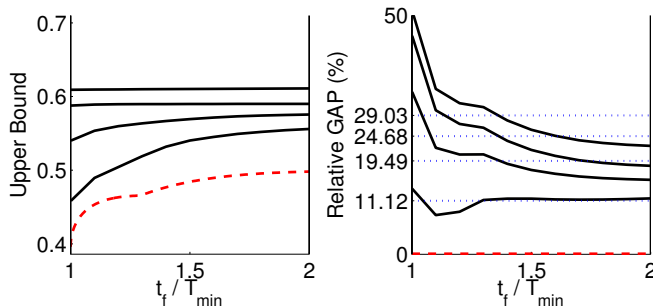


Fig. 5: *lmi*: Blood case, relaxations 2 to 5

IV. CONCLUSION

On this contrast problem, the direct method is an interesting alternative to regularization techniques for initializing

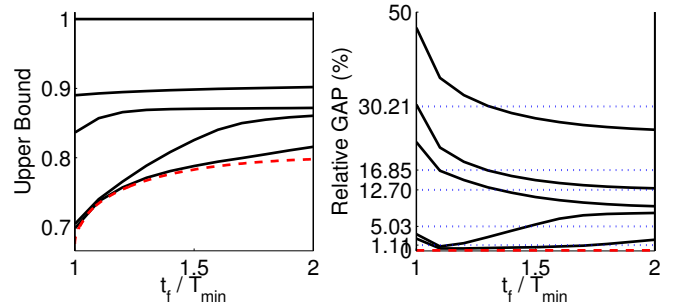


Fig. 6: *lmi*: Fluid case, relaxations 1 to 5

the indirect shooting. Despite the many local optima, *Bocop* often provides solutions close to the global optimum, in a more straightforward way than *HamPath*. However, the direct solutions are less accurate, thus it is preferable to refine them with the indirect method. The *lmi* techniques give an estimate of the global optimum that confirms the optimal results obtained with the indirect methods in [6].

REFERENCES

- [1] P. R. Amestoy, I. S. Duff, J. Koster & J.-Y. L. Excellent. *A fully asynchronous multifrontal solver using distributed dynamic scheduling*, SIAM Journal of Matrix Analysis and Applications, **23** (2001), no. 1, 15–41.
- [2] F. J. Bonnans, P. Martinon & V. Grélaud. *Bocop - A collection of examples*, Technical report, INRIA, 2012. RR-8053.
- [3] B. Bonnard, M. Chyba & J. Mariott, *Singular trajectories and the contrast imaging problem in nuclear magnetic resonance*, SIAM J. Control Optim., to appear, (2013).
- [4] B. Bonnard & O. Cots, *Geometric numerical methods and results in the control imaging problem in nuclear magnetic resonance*, Math. Models Methods Appl. Sci., to appear, (2012).
- [5] B. Bonnard, O. Cots, S. Glaser, M. Lapert, D. Sugny & Y. Zhang, *Geometric optimal control of the contrast imaging problem in nuclear magnetic resonance*, IEEE Trans. Automat. Control, **57** (2012), no. 8, 1957–1969.
- [6] O. Cots, *Contrôle optimal géométrique : méthodes homotopiques et applications*. Phd thesis, Institut Mathématiques de Bourgogne, Dijon, France, 2012.
- [7] D. Henrion, J. B. Lasserre & J. Löfberg, *GloptiPoly 3: Moments, Optimization and Semidefinite Programming*, Optim. Methods and Software, **24** (2009), no. 4-5, 761–779.
- [8] N. Khaneja, T. Reiss, C. Kehlet, T. Schulte-Herbrüggen & S. J. Glaser, *Optimal control of coupled spin dynamics: design of NMR pulse sequences by gradient ascent algorithms*, J. of Magn. Reson., **172** (2005), 296–305.
- [9] M. Lapert, Y. Zhang, M. Janich, S. J. Glaser & D. Sugny, *Exploring the physical limits of saturation contrast in Magnetic Resonance Imaging* Sci. Rep. **2**, 589 (2012).
- [10] J. B. Lasserre, *Positive polynomials and their applications*, Imperial College Press, London, 2009.
- [11] J. B. Lasserre, D. Henrion, C. Prieur & E. Trélat, *Nonlinear optimal control via occupation measures and LMI relaxations*, SIAM J. Control Opt., **47** (2008), no. 4, 1643–1666.
- [12] M. H. Levitt, *Spin dynamics: basics of nuclear magnetic resonance*, John Wiley and sons, Ney York-London-Sydney, 2008
- [13] J.F. Sturm, *Using SeDuMi 1.02, a MATLAB toolbox for optimization over symmetric cones*, Optimization Methods and Software **11-12** (1999), 625-653. Special issue on Interior Point Methods (CD supplement with software).
- [14] A. Wächter & L.T. Biegler. *On the implementation of a primal-dual interior point filter line search algorithm for large-scale nonlinear programming*, Mathematical Programming, **106** (2006), no. 1, 25–57.